Bioconjugate Chemistry

pubs.acs.org/bc

Communication

Self-Regulating Hydrogel Driven by Light-Responsive Glyco-Supramolecular Reassembly

Shun Yao, Zhen Zhao, Chunsen Zhao, Junjie Li, Feng Wang,* and Sami Halila*

Cite This: https://doi.org/10.1021/acs.bioconjchem.5c00626

Read Online

ACCESS | Metrics & More | Article Recommendations | Supporting Information

ABSTRACT: Light-responsive supramolecular materials that operate autonomously represent a key step toward smart, energy-efficient systems. Yet, achieving intrinsic reversibility without external triggers is rare. Here, we present two azobenzene−glycoconjugate amphiphiles bearing glucose (Glc-Azo) or maltose (Mal-Azo) headgroups whose supramolecular organization is dictated by carbohydrate-mediated interactions. Both derivatives undergo efficient *trans*−*cis* photoisomerization under UV irradiation. Remarkably, when assembled in aqueous media, they autonomously revert to the *trans* configuration in the dark without external thermal input. This self-recovery is attributed to a hydrogen-bond-rich glycosidic microenvironment that modulates azobenzene packing and promotes structural reorganization. Incorporation of the bulkier maltose moiety affords robust, thermoreversible supramolecular hydrogels that undergo fully reversible, light-induced gel−sol transitions—dissociating upon UV exposure and spontaneously reassembling thereafter. These results reveal the power of glyco-directed supramolecular architectures to enable autonomous, energy-efficient photoresponsive soft materials, with implications for biomedical and smart-material applications.

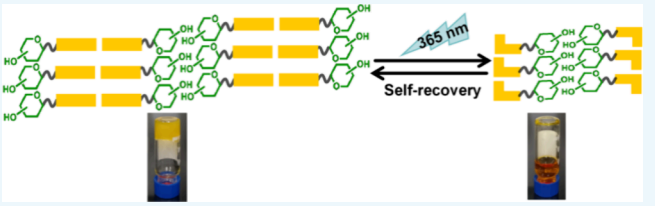

INTRODUCTION

Sugar-based molecular building blocks are increasingly exploited in supramolecular materials design owing to their intrinsic biocompatibility, high hydrophilicity, and exceptional hydrogen-bonding capability.[1−4] These attributes enable programmable assembly of nanostructures with diverse morphologies (fibers, sheets, spheres, ...) and underpin broad biomedical utility.[5−10] Building on these properties, we previously established a protection-free synthetic strategy for sugar-based amphiphiles, enabling multifunctional systems that exhibit self-assembling hydrogelation, enzyme-induced hydrogelation, specific lectin (LecA) recognition, and antimicrobial behavior.[11−15] Beyond these inherent advantages, the structural and chemical versatility of carbohydrates provides a robust platform for engineering stimuli-responsive molecular systems.[16−19]

Azobenzene is a canonical molecular photoswitch that undergoes *trans*-to-*cis* photoisomerization under light,[20−23] a property widely harnessed to modulate supramolecular assembly.[24−27] For example, host−guest interactions between azobenzene derivatives and cyclodextrins have yielded hydrogels with reversible phase transitions under alternating visible light,[28] and amphiphilic azobenzenes embedded in plasma membranes can drive rapid, reversible optical control of cell surface area.[29] Glycosylated azobenzenes similarly display photoresponsive behavior in aqueous media, enabling light-triggered morphological transitions among assembled states.[30−33]

Despite substantial progress, most reversible photoisomerization cycles in amphiphilic azobenzene systems rely on external stimuli (heat or secondary light inputs), limiting operational autonomy and practical utility. The ability of glyco-supramolecular assemblies to confine azobenzene units within dynamic, geometrically constrained microenvironments—thereby enabling self-recovery after photoisomerization without auxiliary input—remains underexplored. Such intrinsic reversibility, orchestrated by the supramolecular microenvironment, offers a route to autonomous, energy-efficient photoresponsive materials. When embedded in hydrogels, this self-sustaining photoresponse is particularly attractive for developing advanced self-regulating materials.[34]

Here, we report the design and synthesis of two azobenzene−glycoconjugates, Glc-Azo and Mal-Azo, using glucose and maltose as hydrophilic moieties (Figure 1a). We systematically investigated their self-assembly and photoresponsive properties, with emphasis on the contribution of sugar-mediated aggregation to spontaneous *cis*-to-*trans* recovery in the assembled state. Guided by this behavior, we strategically tuned the molecular architecture from Glc-Azo to

Received: December 12, 2025
Revised: March 4, 2026
Accepted: March 9, 2026

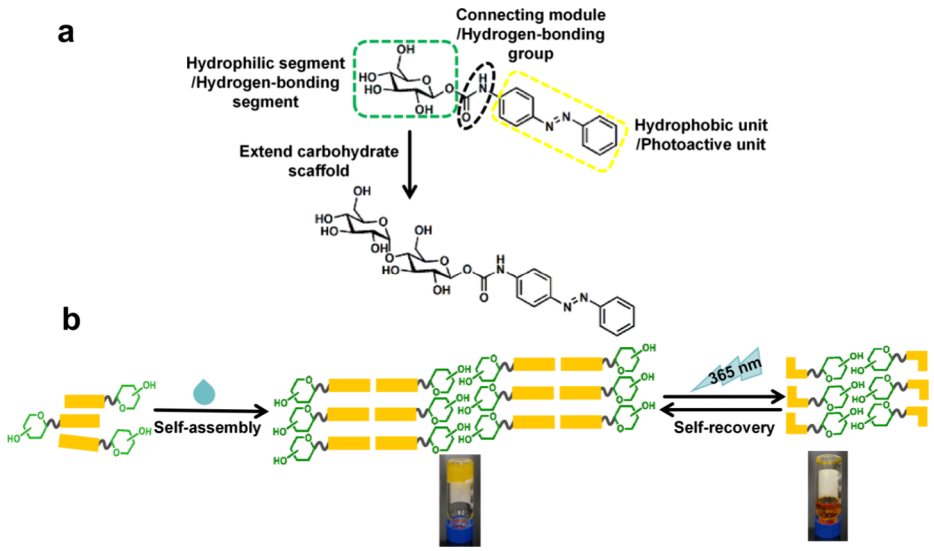

Figure 1. (a) Rational design and chemical structures of the Glc-Azo and Mal-Azo molecules. (b) Schematic of their self-assembly process and photoresponsive behavior.

Mal-Azo to create an autonomous, reversible supramolecular hydrogel (Figure 1b). These results highlight the dual role of glycosidic scaffolds in enhancing material properties and enabling novel photochemical responses in integrated molecular switches, thereby informing the design of next-generation photoresponsive biomaterials.

RESULTS AND DISCUSSION

Synthesis of Azobenzene Glycosides

Azobenzene glycoconjugates were accessed via carbamate linkage formation between azobenzene and sugar units. First, 4-aminoazobenzene was converted to the corresponding isocyanate using triphosgene (1.2 equiv) under anhydrous conditions. Subsequent nucleophilic addition to 2,3,4,6-tetra-*O*-acetyl-D-glucopyranose and 2,3,6,2',3',4',6'-hepta-*O*-acetyl-maltose, in the presence of triethylamine, afforded the respective glycosyl carbamates with high β-selectivity, as indicated by the anomeric proton coupling constant (Supporting Information (SI)). Orthogonal deprotection with aqueous ammonia (pH 9−10, ice-bath) followed by column chromatography furnished Glc-Azo and Mal-Azo. Structures were confirmed by NMR spectroscopy, mass spectrometry, and IR spectroscopy.

Supramolecular Self-Assembly in Glc-Azo

The assembly behavior of Glc-Azo was first examined spectroscopically in dilute solution. In DMSO (5×10^{-5} M), the UV−Vis spectrum displayed bands at 258, 358, and 450 nm; the latter two were assigned to $\pi-\pi^*$ and $n-\pi^*$ transitions of the azobenzene unit,[35−37] respectively (Figure 2a). To assess aggregation, spectra were recorded in DMSO−water mixtures with increasing water fractions. As water content increased, the 358 nm band progressively blue-shifted. The observed 12 nm shift from pure DMSO to pure water is a clear signal for the formation of supramolecular H-aggregates in the aqueous medium (Figure 2b).

Given its self-assembly in water, gelation was evaluated by vial inversion. Due to low solubility at room temperature, Glc-Azo required intensive heating to dissolve. Although gelation occurred upon cooling at 3 wt % (Figure S13a), the resulting gel did not withstand repeated thermal cycles, likely due to molecular degradation induced by excessive heating. Transmission electron microscopy (TEM) revealed sheet-like nanostructures with nonuniform dimensions in aqueous solution (Figure S13b).

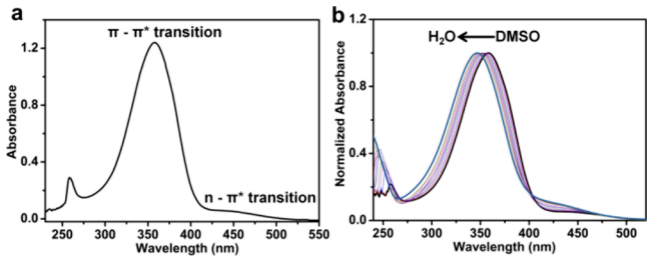

Figure 2. (a) UV−Vis absorption of Glc-Azo (5×10^{-5} M) in DMSO and (b) normalized spectra with increasing water fraction.

To probe azobenzene interactions during assembly, solvent-dependent ^{1}H NMR spectra were collected at room temperature by varying the DMSO-d_6/D_2O ratio (2×10^{-2} M) (Figure 3).[38] Amide and sugar hydroxyl protons were not observed due to rapid exchange with the solvent, confirmed by complete disappearance upon addition of 20% D_2O.[39] Increasing D_2O content up to 70%, where precipitation occurred, induced weak upfield shifts of aromatic signals (Hb/Hc, Ha, Hd/He), ultimately coalescing into composite resonances. These data suggest a non−closely packed azobenzene arrangement with minimal $\pi-\pi$ stacking in the assembled state.

To further elucidate the noncovalent packing mode, single crystals of Glc-Azo suitable for X-ray diffraction were grown from DMSO/water (2:3 v/v). The single-crystal structure provides a reference model for intermolecular interactions and packing tendencies, although the actual arrangement in aqueous assemblies may differ. The corresponding crystallographic parameters are summarized in Table S1, and key intermolecular interactions are illustrated in Figure 4. The solid-state structure revealed one-dimensional chains stabilized by intermolecular hydrogen bonds between adjacent sugar units (O7···H6, d = 1.8040 Å) together with very weak C−H···H−C contacts among azobenzene units (H4A···H4A, d =

https://doi.org/10.1021/acs.bioconjchem.5c00626
Bioconjugate Chem. XXXX, XXX, XXX−XXX

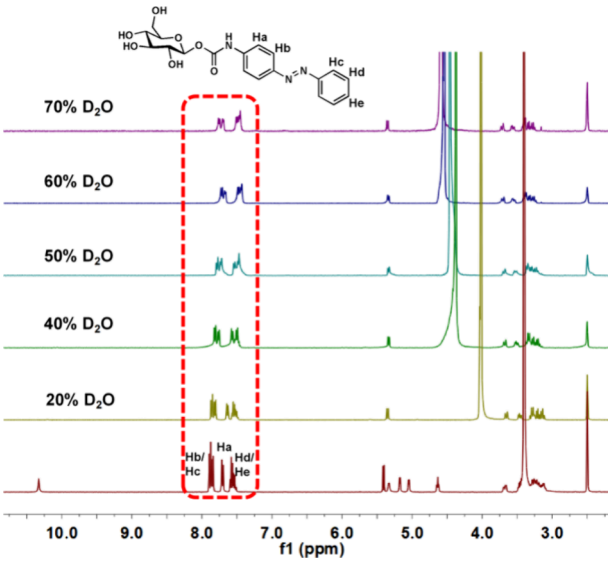

Figure 3. Solvent-dependent ^{1}H NMR spectra of Glc-Azo (2×10^{-2} M) in DMSO-d_6/D_2O with varying volume ratios.

2.3974 Å) (Figure 4a). Chains interconnected via hydrogen bonds (O7···H6, d = 1.8040 Å; O4···H3, d = 1.9716 Å) formed two-dimensional layers (Figure 4b). No intralayer $\pi-\pi$ stacking between azobenzenes was detected; vertical ring distances (2.0594 Å and 1.7715 Å) and slip angles (69.852° and 72.767°) fall well outside the typical $\pi-\pi$ stacking regime (Figure S14). By contrast, weak interlayer $\pi-\pi$ interactions (3.6590 and 3.5637 Å; slip angles 13.718° and 18.903°) linked the layers into a three-dimensional network (Figures 4c and 4d), consistent with the solvent-dependent NMR observations.

Photoresponsive Behavior of Glc-Azo

The photoresponsive properties of Glc-Azo were evaluated using UV−Vis spectroscopy, ^{1}H NMR, and TEM for comprehensive analysis. In the monomeric state (DMSO, 5×10^{-5} M), 365 nm irradiation increased absorption at 258 and 450 nm without significant shifts, while the 358 nm band decreased and blue-shifted by 42 nm, reaching a photostationary state within seconds (Figure 5a). In the dark, only marginal *cis*-to-*trans* recovery occurred over 2 h (Figure S15). Upon heating to 75 °C, the UV−Vis spectrum gradually reverted over time and was nearly fully restored within 1.5 h (Figure 5b), indicating that while the molecules can undergo photoisomerization in solution, the efficient reversion from the *cis* to the *trans* conformation required thermal energy. The photoresponse was further supported by ^{1}H NMR spectroscopy (Figure 5c). In DMSO-d_6 (2×10^{-2} M), prolonged 365 nm irradiation induced pronounced upfield shifts of the amide (10.33 to 10.03 ppm) and aromatic protons (region of 7.90 to 7.51 ppm), consistent with *trans*-to-*cis* conversion (~95% by ^{1}H NMR). Subsequent thermal treatment returned all signals to their initial positions, confirming excellent thermal reversibility.

In self-assembled state in water (5×10^{-5} M), Glc-Azo remained photoactive and underwent *trans*-to-*cis* isomerization upon 365 nm irradiation, as evidenced by rapid spectral changes (intensity increase and slight red shift at ~235 nm; intensity decrease and 26 nm blue shift at ~346 nm; sharpening at ~438 nm) (Figure S16a). Notably, in the assembled state the system spontaneously recovered to the *trans* configuration in the dark without heating, achieving near-complete restoration within ~40 min (Figure S16b). This self-recovery contrasts sharply with the behavior of Glc-Azo in DMSO solution, which showed no significant recovery even after standing for 2 h under identical test conditions. The absence of recovery in the molecularly dissolved state further confirms that the self-recovery observed in the assembled system is not thermally driven. Moreover, the assembled system exhibited high reversibility over eight consecutive irradiation−recovery cycles without apparent fatigue (Figure

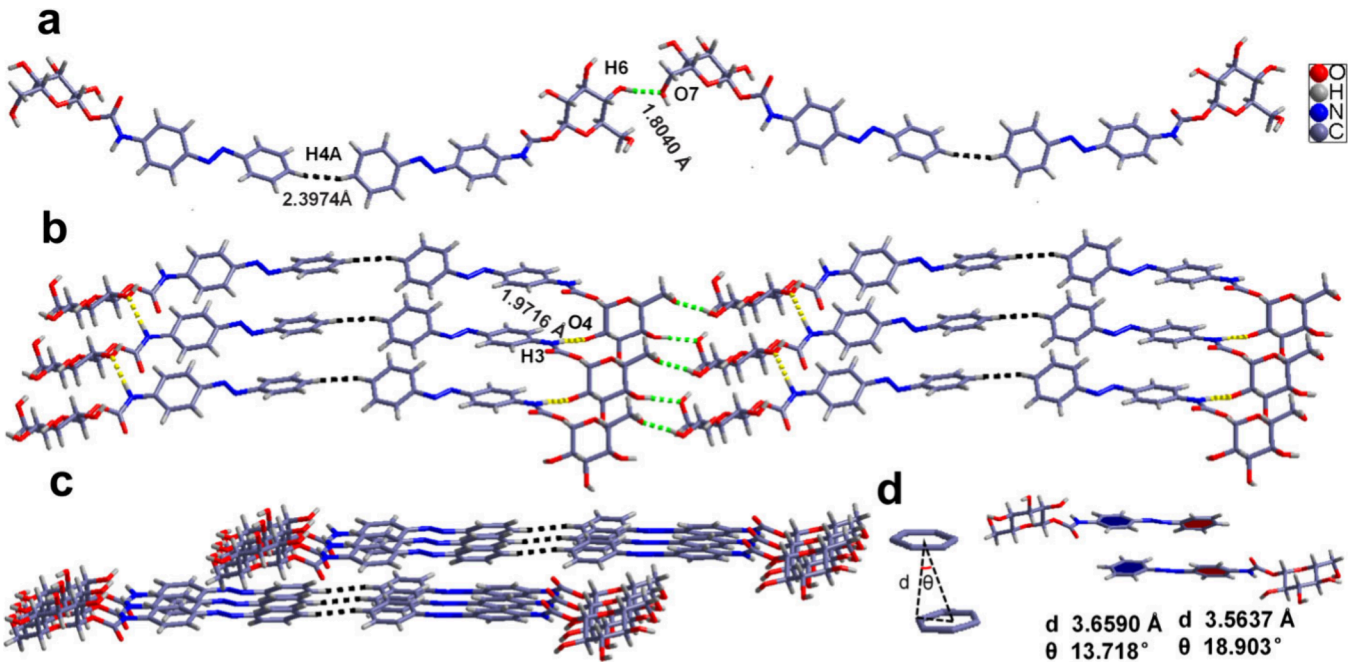

Figure 4. Crystal structure of Glc-Azo showing (a) 1D chain formation, (b) 2D sheet assembly and (c) packing arrangement between the layered structures. (d) π-π stacking interactions.

https://doi.org/10.1021/acs.bioconjchem.5c00626
Bioconjugate Chem. XXXX, XXX, XXX−XXX

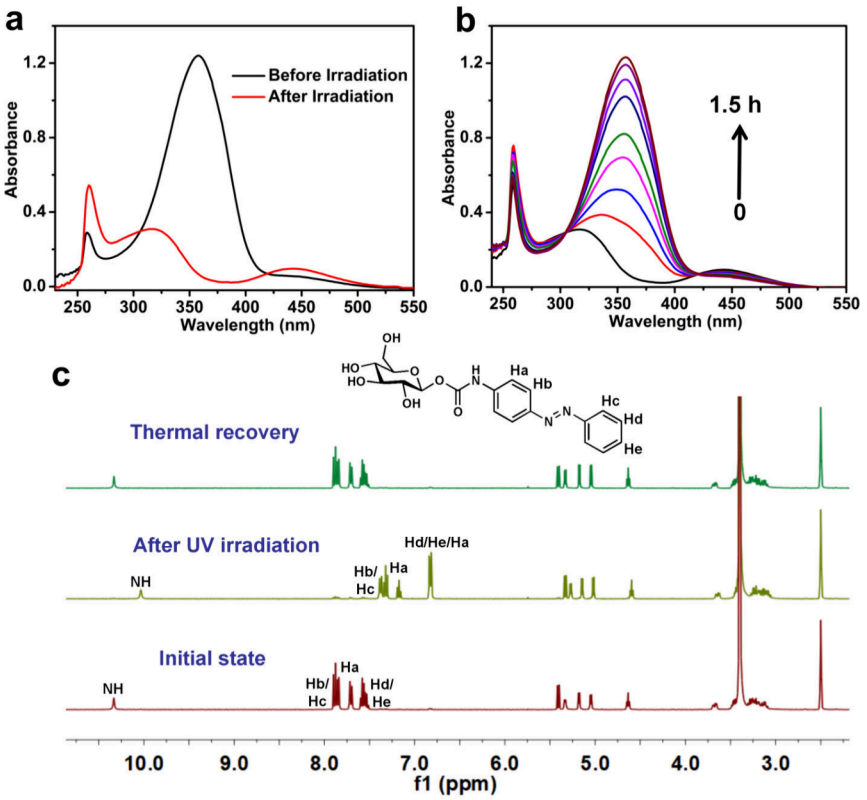

Figure 5. Investigation of the photoresponse of Glc-Azo (5×10^{-5} M) in DMSO. (a) UV−Vis spectra before and after 365 nm light irradiation. (b) Complete recovery of the UV−Vis absorption upon heating at 75 °C for 1.5 h. (c) ^{1}H NMR spectra of Glc-Azo (2×10^{-2} M in DMSO-d_6) showing reversible photoisomerization: initial state, after 365 nm irradiation, and following thermal recovery.

S16c). Nevertheless, upon prolonged 365 nm irradiation, the hydrogel underwent collapse into a precipitate and could not be reconstituted even upon heating. This indicates that the inherent limitations of the hydrogel itself prevented reversible macroscopic gel−sol transition under such conditions.

To elucidate self-recovery, UV−Vis spectra in DMSO and water after 365 nm irradiation showed blue shifts of the 261 and 442 nm bands to 248 and 431 nm, respectively, while the 316 nm band remained largely unchanged (Figure S17a), suggesting formation of a distinct assembled morphology postirradiation. TEM revealed smaller nanostructures (~200 nm length, ~300 nm width) compared to preirradiation assemblies (Figure S17b). We infer that weak azobenzene−azobenzene interactions in Glc-Azo permit configurational changes under UV light that disrupt H−H contacts and modest $\pi-\pi$ interactions without dismantling the hydrogen-bond network. Self-recovery reflects the system's relaxation to a global energy minimum, wherein the hydrogen-bond-rich glyco-supramolecular matrix preferentially stabilizes *trans*-azobenzene assemblies.

Supramolecular Self-Assembly and Hydrogel Formation in Mal-Azo

To improve the hydrogel property and overcome the irreversible UV-induced collapse observed in Glc-Azo, we introduced maltose, a disaccharide containing a higher number of hydroxyl groups, to simultaneously enhance hydrogen-bonding capacity and hydration. This structural modification creates a robust yet dynamic glycosidic environment that effectively confines the azobenzene units. The designed structure is intended to achieve an optimal balance between structural integrity−ensuring stable gelation−and favorable self-assembly and photoresponsive properties, culminating in the successful development of Mal-Azo. In DMSO, Mal-Azo exhibited UV−Vis bands analogous to Glc-Azo (258, 358, 450 nm) and a 12 nm blue shift of the 358 nm band upon transfer to water (Figure S18), indicative of H-aggregates in water.

Unlike Glc-Azo, Mal-Azo formed a stable, thermoreversible hydrogel at 1.2 wt % after ultrasonication or standing (Figure 6a). The hydrogel remained intact for weeks and underwent

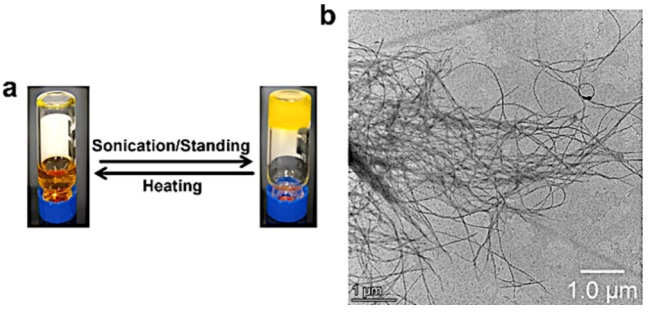

Figure 6. (a) Photographs demonstrating thermoreversible sol−gel transition and (b) TEM image revealing a nanofibrillar network responsible for gelation.

multiple thermoreversible sol−gel cycles (Figure S19). TEM showed an interconnected network of micrometer-length nanofibers (~25 nm width) (Figure 6b). Solvent-dependent ^{1}H NMR revealed tighter molecular packing than in Glc-Azo: at 70% D_2O, distinct upfield shifts and signal changes of azobenzene protons indicated enhanced $\pi-\pi$ stacking without precipitation (Figure S20).

https://doi.org/10.1021/acs.bioconjchem.5c00626
Bioconjugate Chem. XXXX, XXX, XXX−XXX

Photoresponsive Behavior and Self-Regulating Hydrogel of Mal-Azo

The photoisomerization properties of Mal-Azo were thoroughly investigated in both molecular and assembled states. In DMSO, Mal-Azo underwent efficient *trans*-to-*cis* photoisomerization under 365 nm irradiation (~95% by ^{1}H NMR). Thermal recovery required heating to 75 °C and occurred over ~1.5 h (Figures S21 and S22). In aqueous assemblies, Mal-Azo displayed spontaneous *cis*-to-*trans* recovery within ~40 min without heating and maintained excellent reversibility over eight irradiation−recovery cycles without fatigue (Figures 7a−7c). Although the exact proportion of the *cis* isomer in the photostationary state could not be precisely quantified, this conclusion is clearly supported by the observed UV−Vis spectral changes and the corresponding recovery behavior. Postirradiation characterization indicated that Mal-Azo remained assembled, undergoing morphological transitions from nanofibers to fragmented structures (Figure S23).

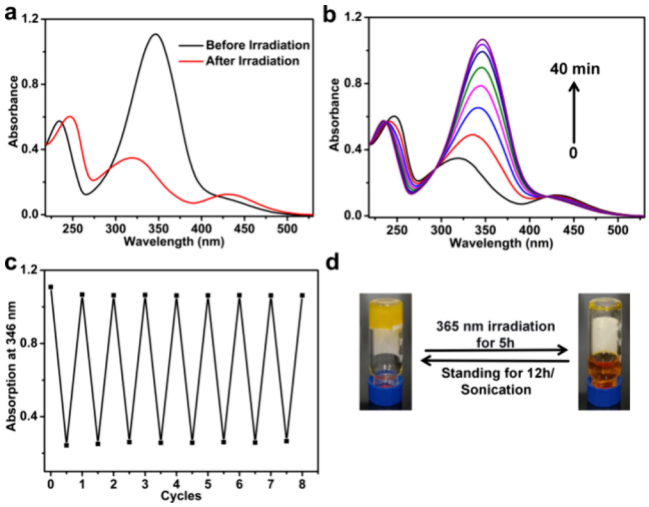

Figure 7. Photoresponsive behavior of Mal-Azo in water (5×10^{-5} M). (a) UV−Vis spectral evolution under 365 nm irradiation, indicating the occurrence of photoisomerization. (b) Self-recovery of the absorption spectrum to its initial state within 40 min in the dark after irradiation. (c) Reversible switching over 8 consecutive cycles, demonstrating excellent repeatability and cycling stability. (d) Illustration of the reversible gelation behavior, showing photo-triggered dissolution, subsequent spontaneous reformation in the dark (12 h, 25 °C), and rapid gelation via ultrasonication.

The combination of photoresponsive behavior and self-recovery enabled a self-regulating hydrogel system. Upon extended UV irradiation (5 h), the Mal-Azo hydrogel underwent complete dissolution into a sol state. Crucially, it spontaneously reassembled into a stable gel after 12 h in the dark at 25 °C without external intervention, and gelation occurred rapidly when assisted by ultrasonication (Figure 7d). Quantitative rheological measurements were attempted on the Mal-Azo hydrogel before irradiation and after self-recovery, but the obtained modulus data were not reproducible and fell below the reliable detection limit due to the very weak mechanical strength of the gel. This fully reversible, photo-controlled sol−gel transition originated from the unique glyco-supramolecular microenvironment, which provided optimal spatial confinement while maintaining structural flexibility. The hydrogen-bond-rich glycoside matrices facilitated self-recovery of the *trans* configuration, enabling supramolecular network reconstruction. This autonomous self-regulating characteristic established Mal-Azo as a promising smart material platform for biomedical applications requiring spatiotemporal control and repair capabilities.[40]

CONCLUSIONS

The glyco-supramolecular microenvironment plays a decisive role in orchestrating the photobehavior of azobenzene conjugates. Carbohydrate-driven self-assembly templates nanostructure formation and confers autonomous function by facilitating spontaneous *cis-to-trans* recovery postirradiation. Strategic expansion of the sugar unit from glucose (Glc-Azo) to maltose (Mal-Azo) enabled fabrication of a stable supramolecular hydrogel capable of fully reversible, light-regulated gel−sol transitions. The observed autonomy and self-regulation underscore the potential of sugar-directed interactions to encode life-like properties—adaptivity and autonomy—into synthetic materials, providing a robust foundation for next-generation energy-efficient, stimuli-responsive biomaterials.

EXPERIMENTAL SECTION

Synthesis of Compound Glc-Azo

The specific synthetic route of Glc-Azo is shown in Scheme S1. The compounds Glc-OAc and Glc-OAc-OH were synthesized according to the literature.[41]

Synthesis of Glc-OAc-Azo. To a solution of triphosgene (2.4 mmol) in dry dichloromethane (DCM, 20 mL) under nitrogen was added a solution of 4-aminoazobenzene (2.0 mmol) in dry DCM. Dry triethylamine (5 mL) was then added dropwise. The resulting mixture was stirred at room temperature for 30 min, after which 2,3,4,6-tetra-*O*-acetyl-D-glucopyranose (Glc-OAc, 2.0 mmol) was added. Upon reaction completion, the mixture was diluted with DCM (40 mL) and washed with water (2 × 100 mL). The organic layer was dried over anhydrous Na_2SO_4, filtered, and concentrated in vacuo. The residue was purified by flash column chromatography on silica gel (DCM/EtOAc, 10:1 v/v) to afford Glc-OAc-Azo as a yellow solid. Yield: 55%, ^{1}H NMR ($CDCl_3$, 400 MHz, ppm) δ 7.93−7.88 (m, 4H), 7.56−7.43 (m, 5H), 7.16 (s, 1H), 5.79 (d, J = 8.2 Hz, 1H), 5.32 (t, J = 9.4 Hz, 1H), 5.23−5.14 (m, 2H), 4.34 (dd, J = 12.6, 4.5 Hz, 1H), 4.15 (dd, J = 12.5, 1.9 Hz, 1H), 3.93−3.89 (m, 1H), 2.09−2.03 (m, 12H). ^{13}C NMR (101 MHz, $CDCl_3$) δ 170.8, 170.3, 169.8, 169.7, 152.8, 150.7, 149.2, 139.5, 131.1, 129.3, 124.3, 123.0, 119.0, 93.2, 72.9, 72.8, 70.3, 61.7, 20.9, 20.8. MS (APCI) m/z: calcd for $[M + H]^+$, 572.1875; found, 572.1872. FT-IR (cm^{-1}): 3387, 1740, 1597, 1528, 1366, 1223, 1066, 1034, 843, 687, 548.

Synthesis of Glc-Azo. A solution of Glc-OAc-Azo (1.0 mmol) in methanol (MeOH, 30 mL) was treated dropwise with ammonium hydroxide until pH 9 was reached. The reaction mixture was stirred at 0 °C for 12 h. The solvent was removed by rotary evaporation, and the crude product was purified by flash column chromatography on silica gel (EtOAc/MeOH, 8:2 v/v) to afford Glc-Azo as a yellow solid. Yield: 65%, ^{1}H NMR (DMSO-d_6, 400 MHz, ppm) δ 10.33 (s, 1H), 7.90−7.84 (m, 4H), 7.71 (d, J = 8.9 Hz, 2H), 7.60−7.51 (m, 3H), 5.42 (d, J = 8.1 Hz, 1H), 5.32 (d, J = 5.2 Hz, 1H), 5.16 (d, J = 4.9 Hz, 1H), 5.03 (d, J = 5.5 Hz, 1H), 4.62 (t, J = 5.9 Hz, 1H), 3.70−3.66 (m, 1H), 3.49−3.43 (m, 1H), 3.32−3.10 (m, 4H). ^{13}C NMR (101 MHz, DMSO-d_6) δ 152.1, 147.4, 142.0, 131.0, 129.4, 123.8, 122.3, 118.6, 95.3, 77.8, 76.7, 72.5, 69.6, 60.6. MS (APCI) m/z: calcd for $[M + H]^+$, 404.1452; found, 404.1459. FT-IR (cm^{-1}): 3278, 1741, 1597, 1540, 1411, 1310, 1219, 1065, 1020, 843, 683, 541.

Synthesis of Compounds Mal-Azo

The specific synthetic route of Mal-Azo is shown in Scheme S2. The compounds Mal-OAc and Mal-OAc-OH were synthesized according to the literature.[42,43] The synthesis methods of Mal-OAc-Azo and

https://doi.org/10.1021/acs.bioconjchem.5c00626
Bioconjugate Chem. XXXX, XXX, XXX−XXX

Mal-Azo were the same as that of Glc-OAc-Azo and Glc-Azo, respectively.

Mal-OAc-Azo, yellow solid, yield: 70%, ^{1}H NMR ($CDCl_3$, 400 MHz, ppm) δ 7.93−7.88 (m, 4H), 7.55−7.45 (m, 5H), 7.08 (s, 1H), 5.80 (d, J = 8.2 Hz, 1H), 5.42−5.33 (m, 3H), 5.06 (q, 2H), 4.87 (dd, J = 10.5, 4.0 Hz, 1H), 4.48 (dd, J = 12.3, 2.3 Hz, 1H), 4.29−4.22 (m, 2H), 4.10−4.04 (m, 2H), 3.97−3.87 (m, 2H), 2.13−2.00 (m, 21H). ^{13}C NMR (101 MHz, $CDCl_3$) δ 170.8, 170.7, 170.2, 170.1, 169.7, 152.8, 150.6, 149.2, 139.5, 131.1, 129.3, 124.3, 123.0, 119.0, 95.9, 92.8, 75.4, 73.2, 72.6, 71.0, 70.2, 69.5, 68.8, 68.2, 62.7, 61.6, 21.1, 21.0, 20.9, 20.8. MS (ESI) m/z: calcd for $[M + Na]^+$, 882.2539; found, 882.2565. FT-IR (cm^{-1}): 3294, 1740, 1597, 1540, 1369, 1308, 1227, 1031, 853, 687, 553.

Mal-Azo, yellow solid, yield: 68%, ^{1}H NMR (DMSO-d_6, 400 MHz, ppm) δ 10.35 (s, 1H), 7.90−7.84 (m, 4H), 7.71 (d, J = 8.9 Hz, 2H), 7.60−7.53 (m, 3H), 5.66 (d, J = 3.2 Hz, 1H), 5.51−5.44 (m, 3H), 5.06 (d, J = 3.7 Hz, 1H), 4.92 (q, 2H), 4.61 (t, J = 5.9 Hz, 1H), 4.53 (t, J = 5.5 Hz, 1H), 3.71 (q, 1H), 3.65−3.57 (m, 3H), 3.51−3.40 (m, 5H), 3.29−3.23 (m, 2H), 3.11−3.05 (m, 1H). ^{13}C NMR (101 MHz, DMSO-d_6) δ 152.1, 152.0, 147.4, 142.0, 131.1, 129.5, 123.8, 122.3, 118.6, 100.8, 95.1, 78.9, 76.3, 76.0, 73.5, 73.3, 72.5, 72.1, 69.9, 60.8, 60.2. MS (ESI) m/z: calcd for $[M + Na]^+$, 588.1800; found, 588.1824. FT-IR (cm^{-1}): 3294, 1726, 1600, 1548, 1309, 1225, 1021, 842, 764, 685, 546.

No unexpected or unusually high safety hazards were encountered in this work.

■ ASSOCIATED CONTENT

Supporting Information

The Supporting Information is available free of charge at https://pubs.acs.org/doi/10.1021/acs.bioconjchem.5c00626.

Materials and instruments. synthetic routes and characterization (NMR, MS) of azo benzene glycosides, supplementary data on self-assembly and photoresponse, and crystallographic parameters (PDF)

■ AUTHOR INFORMATION

Corresponding Authors

Sami Halila − *Centre for Organic and Nanohybrid Electronics, Silesian University of Technology, Gliwice 44-100, Poland; Univ. Grenoble Alpes, CNRS, CERMAV, Grenoble 38000, France;* orcid.org/0000-0002-9673-1099; Email: sami.halila@cermav.cnrs.fr

Feng Wang − *CAS Key Laboratory of Soft Matter Chemistry, Department of Polymer Science and Engineering, University of Science and Technology of China, Hefei, Anhui 230026, P. R. China;* orcid.org/0000-0002-3826-5579; Email: drfwang@ustc.edu.cn

Authors

Shun Yao − *Biomass Oligosaccharides Engineering Technology Research Center of Anhui Province, Engineering Research Center of Biomass Conversion and Pollution Prevention of Anhui Educational Institutions, School of Chemistry and Materials Engineering, Fuyang Normal University, Fuyang 236037, P. R. China*

Zhen Zhao − *Biomass Oligosaccharides Engineering Technology Research Center of Anhui Province, Engineering Research Center of Biomass Conversion and Pollution Prevention of Anhui Educational Institutions, School of Chemistry and Materials Engineering, Fuyang Normal University, Fuyang 236037, P. R. China*

Chunsen Zhao − *Biomass Oligosaccharides Engineering Technology Research Center of Anhui Province, Engineering Research Center of Biomass Conversion and Pollution Prevention of Anhui Educational Institutions, School of Chemistry and Materials Engineering, Fuyang Normal University, Fuyang 236037, P. R. China*

Junjie Li − *Biomass Oligosaccharides Engineering Technology Research Center of Anhui Province, Engineering Research Center of Biomass Conversion and Pollution Prevention of Anhui Educational Institutions, School of Chemistry and Materials Engineering, Fuyang Normal University, Fuyang 236037, P. R. China*

Complete contact information is available at: https://pubs.acs.org/10.1021/acs.bioconjchem.5c00626

Author Contributions

The manuscript was written through contributions of all authors, and all authors have given approval to the final version of the manuscript.

Notes

The authors declare no competing financial interest.

■ ACKNOWLEDGMENTS

We acknowledge the financial support from the Institut Carnot PolyNat (ANR-21-CARN-0025-0) and the PhD Research Start-up Foundation of Fuyang Normal University (No. 2025KYQD0189). We also acknowledge the support of the French Agence Nationale de la Recherche (ANR), under grant ANR-21-CE07-0050 (SWEET-DISPLAY). We thank CBH-EUR-GS (ANR-17-EURE-0003) and Glyco@Alps (ANR-15-IDEX-02) for additional support.

■ REFERENCES

(1) Delbianco, M.; Bharate, P.; Varela-Aramburu, S.; Seeberger, P. H. Carbohydrates in supramolecular chemistry. *Chem. Rev.* **2016**, *116* (4), 1693−1752.

(2) Datta, S.; Bhattacharya, S. Multifarious facets of sugar-derived molecular gels: molecular features, mechanisms of self-assembly and emerging applications. *Chem. Soc. Rev.* **2015**, *44* (15), 5596−5637.

(3) Su, L.; Feng, Y. L.; Wei, K. C.; Xu, X. Y.; Liu, R. Y.; Chen, G. S. Carbohydrate-based macromolecular biomaterials. *Chem. Rev.* **2021**, *121* (18), 10950−11029.

(4) Wang, B.; Liu, S. J.; Li, H. T.; Dong, W. D.; Liu, H. Y.; Zhang, J.; Tian, C.; Dong, S. W. Facile preparation of carbohydrate-containing adjuvants based on self-assembling glycopeptide conjugates. *Angew. Chem., Int. Ed.* **2024**, *63* (1), No. e202309140.

(5) Liu, Y. C.; Liu, G. J.; Zhou, W.; Feng, G. L.; Ma, Q. Y.; Zhang, Y.; Xing, G. W. In situ self-assembled *J*-aggregate nanofibers of glycosylated Aza-BODIPY for synergetic cell membrane disruption and type I photodynamic therapy. *Angew. Chem., Int. Ed.* **2023**, *62* (40), No. e202309786.

(6) Zhang, J. W.; Feng, G. L.; Niu, X.; Liu, Y. C.; Zhou, W.; Ma, Q. Y.; Liu, G. J.; Zhang, Y.; Xing, G. W. Glycosylated and rhodamine-conjugated tetraphenylethylene: a type I and II reactive oxygen species generator for photodynamic therapy. *Chem. Commun.* **2025**, *61* (16), 3403−3406.

(7) Biswakarma, D.; Dey, N.; Bhattacharya, S. A thermo-responsive supramolecular hydrogel that senses cholera toxin via color-changing response. *Chem. Commun.* **2020**, *56* (56), 7789−7792.

(8) Li, J.-J.; Hu, Y.; Hu, B.; Wang, W.; Xu, H.; Hu, X.-Y.; Ding, F.; Li, H.-B.; Wang, K.-R.; Zhang, X.; Guo, D.-S. Lactose azocalixarene drug delivery system for the treatment of multidrug-resistant pseudomonas aeruginosa infected diabetic ulcer. *Nat. Commun.* **2022**, *13* (1), 6279.

(9) Hu, X. L.; Gan, H. Q.; Gui, W. Z.; Yan, K. C.; Sessler, J. L.; Yi, D.; Tian, H.; He, X. P. Superresolution imaging of antibiotic-induced structural disruption of bacteria enabled by photochromic glyco-

micelles. *Proc. Natl. Acad. Sci. U.S.A.* **2024**, *121* (37), No. e2408716121.
(10) Qi, J.; Yan, Y.; Cheng, B.; Deng, L.; Shao, Z.; Sun, Z.; Li, X. Enzymatic formation of an injectable hydrogel from a glycopeptide as a biomimetic scaffold for vascularization. *ACS Appl. Mater. Interfaces* **2018**, *10* (7), 6180−6189.
(11) Yao, S.; Brahmi, R.; Portier, F.; Putaux, J. L.; Chen, J.; Halila, S. Hierarchical self-assembly of amphiphilic β-C-glycosylbarbiturates into multiresponsive alginate-like supramolecular hydrogel fibers and vesicle hydrogel. *Chem. Eur. J.* **2021**, *27* (67), 16716−16721.
(12) Yao, S.; Brahmi, R.; Bouschon, A.; Chen, J.; Halila, S. Supramolecular carbohydrate-based hydrogels from oxidative hydroxylation of amphiphilic β-*C*-glycosylbarbiturates and α-glucosidase-induced hydrogelation. *Green Chem.* **2023**, *25* (1), 330−335.
(13) Portier, F.; Imberty, A.; Halila, S. Expeditious synthesis of C-glycosyl barbiturate ligands of bacterial lectins: from monomer design to glycoclusters and glycopolymers. *Bioconjugate Chem.* **2019**, *30* (3), 647−656.
(14) Abdallah, A.; Gillon, E.; Rannou, P.; Imberty, A.; Halila, S. Microwave-assisted synthesis of β-N-aryl glycoamphiphiles with diverse supramolecular assemblies and lectin accessibility. *Bioconjugate Chem.* **2024**, *35* (8), 1200−1206.
(15) Chen, B.; Fragal, E. H.; Faudry, E.; Halila, S. In situ growth of silver nanoparticles into reducing-end carbohydrate-based supramolecular hydrogels for antimicrobial applications. *ACS Appl. Mater. Interfaces* **2024**, *16* (51), 70818−70827.
(16) Pires, R. A.; Abul-Haija, Y. M.; Costa, D. S.; Novoa-Carballal, R.; Reis, R. L.; Ulijn, R. V.; Pashkuleva, I. Controlling cancer cell fate using localized biocatalytic self-assembly of an aromatic carbohydrate amphiphile. *J. Am. Chem. Soc.* **2015**, *137* (2), 576−579.
(17) Singh, N.; Lainer, B.; Formon, G. J.; De Piccoli, S.; Hermans, T. M. Re-programming hydrogel properties using a fuel-driven reaction cycle. *J. Am. Chem. Soc.* **2020**, *142* (9), 4083−4087.
(18) Matsumoto, S.; Yamaguchi, S.; Wada, A.; Matsui, T.; Ikeda, M.; Hamachi, I. Photo-responsive gel droplet as a nano-or pico-litre container comprising a supramolecular hydrogel. *Chem. Commun.* **2008**, No. 13, 1545−1547.
(19) Akama, S.; Maki, T.; Yamanaka, M. Enzymatic hydrolysis-induced degradation of a lactose-coupled supramolecular hydrogel. *Chem. Commun.* **2018**, *54* (64), 8814−8817.
(20) Li, Y. R.; Xue, B.; Yang, J. H.; Jiang, J. L.; Liu, J.; Zhou, Y. Y.; Cao, Y.; et al. Azobenzene as a photoswitchable mechanophore. *Nat. Chem.* **2024**, *16* (3), 446−455.
(21) Wu, J. J.; Liu, W. J.; Tang, S. Y.; Wei, S. L.; He, H. W.; Ma, M.; Shi, Y. Q.; Zhu, Y. L.; Chen, S.; Wang, X. Light-Responsive Smart Nanoliposomes: harnessing the azobenzene moiety for controlled drug release under near-infrared Irradiation. *ACS Appl. Mater. Interfaces* **2024**, *16* (42), 56850−56861.
(22) Cheng, H. B.; Zhang, S.; Qi, J.; Liang, X. J.; Yoon, J. Advances in application of azobenzene as a trigger in biomedicine: molecular design and spontaneous assembly. *Adv. Mater.* **2021**, *33* (26), 2007290.
(23) Friedrich, L. M.; Hartke, B.; Lindhorst, T. K. Advancing optoglycomics: two orthogonal azobenzene glycoside antennas in one glycocluster-synthesis, switching cycles, kinetics and molecular dynamics. *Chem. Eur. J.* **2024**, *30* (55), No. e202402125.
(24) Yan, T. F.; Li, F.; Qi, S. W.; Tian, J.; Tian, R. Z.; Hou, J. X.; Luo, Q.; Dong, Z. Y.; Xu, J. Y.; Liu, J. Q. Light-responsive vesicles for enantioselective release of chiral drugs prepared from a supra-amphiphilic M-helix. *Chem. Commun.* **2020**, *56* (1), 149−152.
(25) Yu, B. W.; Liu, J.; Cui, Z. Y.; Wang, C.; Chen, P. P.; Wang, C. T.; Zhang, Y. Z.; Zhu, X. X.; Zhang, Z.; Li, S. C.; Pan, J. H.; Xie, M. Q.; Sheng, H. Z.; Cao, L. X. De novo design of light-responsive protein-protein interactions enables reversible formation of protein assemblies. *Nat. Chem.* **2025**, *17*, 1910.
(26) Yang, J.; Ye, H. J.; Xiang, H. M.; Zhou, X.; Wang, P. Y.; Liu, S. S.; Yang, B. X.; Yang, H. B.; Liu, L. W.; Yang, S. Photo-stimuli smart supramolecular self-assembly of azobenzene/β-Cyclodextrin inclusion complex for controlling plant bacterial diseases. *Adv. Funct. Mater.* **2023**, *33* (42), 2303206.
(27) Tamesue, S.; Takashima, Y.; Yamaguchi, H.; Shinkai, S.; Harada, A. Photoswitchable supramolecular hydrogels formed by cyclodextrins and azobenzene polymers. *Angew. Chem., Int. Ed.* **2010**, *122* (41), 7623−7626.
(28) Fu, Y.; Okuro, K.; Ding, J. D.; Aida, T. Clay Nanosheet-based nanocomposite supramolecular hydrogel enabling rapid, reversible phase transition only with visible light. *Angew. Chem.* **2025**, *137* (4), No. e202416541.
(29) Höglsperger, F.; Vos, B. E.; Hofemeier, A. D.; Seyfried, M. D.; Stövesand, B.; Alavizargar, A.; Topp, L.; Heuer, A.; Betz, T.; Ravoo, B. J. Rapid and reversible optical switching of cell membrane area by an amphiphilic azobenzene. *Nat. Commun.* **2023**, *14* (1), 3760.
(30) Ogawa, Y.; Yoshiyama, C.; Kitaoka, T. Helical assembly of azobenzene-conjugated carbohydrate hydrogelators with specific affinity for lectins. *Langmuir* **2012**, *28* (9), 4404−4412.
(31) Wang, Z. X.; Maisonneuve, S.; Xie, J. One-pot synthesis of water-soluble glycosyl azobenzenes and their photoswitching properties in water. *J. Org. Chem.* **2022**, *87* (24), 16165−16174.
(32) Zhang, J. J.; Ma, W. J.; He, X. P.; Tian, H. Taking orders from light: photo-switchable working/inactive smart surfaces for protein and cell adhesion. *ACS Appl. Mater. Interfaces* **2017**, *9* (10), 8498−8507.
(33) Guo, J. P.; Wang, S. Y.; Yu, Z. H.; Heng, X. Y.; Zhou, N. C.; Chen, G. Well-Defined Oligo (azobenzene-graft-mannose): Photo-stimuli supramolecular self-Assembly and immune effect regulation. *ACS Macro Lett.* **2024**, *13* (3), 273−279.
(34) Guo, K. X.; Yang, X. H.; Zhou, C.; Li, C. Self-regulated reversal deformation and locomotion of structurally homogenous hydrogels subjected to constant light illumination. *Nat. Commun.* **2024**, *15* (1), 1694.
(35) Li, C.; Kazem-Rostami, M.; Seale, J. S.; Zhou, S. L.; Stupp, S. Macroscopic actuation of bisazo hydrogels driven by molecular photoisomerization. *Chem. Mater.* **2023**, *35* (10), 3923−3930.
(36) Wu, S. D.; Chen, Z. Z.; Sun, W. J.; Shi, L. Y. Y.; Shen, A. K.; Cao, J. J.; Liu, Z. T.; Lambert, C. J.; Zhang, H. L. Boosting the photoresponse of azobenzene single-molecule junctions via mechanical interlock and dynamic anchor. *ACS Nano* **2024**, *18* (45), 31547−31558.
(37) Yin, C. C.; Chen, M. N.; Zhang, Z. Y.; Liu, K.; Gao, J. L.; Zhao, X.; Wu, Y. P.; Wang, Y. Light-activated 3D covalent organic framework membranes with adaptive pores for CO_2 recognition and separation. *Sci. Adv.* **2025**, *11* (32), No. eadw8452.
(38) Borsdorf, L.; Herkert, L.; Bäumer, N.; Rubert, L.; Soberats, B.; Korevaar, P. A.; Bourque, C.; Gatsogiannis, C.; Fernández, G. Pathway-controlled aqueous supramolecular polymerization via solvent-dependent chain conformation effects. *J. Am. Chem. Soc.* **2023**, *145* (16), 8882−8895.
(39) Manjarres, A. M.; Albers, A.; Fernandez, G. Photoregulated supramolecular polymerization through halogen bonding. *Angew. Chem., Int. Ed.* **2025**, *137* (7), No. e202419720.
(40) Chung, T.; Choi, J.; Enomoto, T.; Park, S.; Kim, S.; Kim, Y. S. Self-Regulating Hydrogel Actuators. *Chem. Rev.* **2025**, *125* (18), 9053−9088.
(41) Ito, H.; Kamachi, T.; Yashima, E. Specific surface modification of the acetylene-linked glycolipid vesicle by click chemistry. *Chem. Commun.* **2012**, *48* (45), 5650−5652.
(42) Ye, H.; Xiao, C.; Zhou, Q. Q.; Wang, P. G.; Xiao, W. J. Synthesis of phenolic glycosides: glycosylation of sugar lactols with aryl bromides via dual photoredox/Ni catalysis. *J. Org. Chem.* **2018**, *83* (21), 13325−13334.
(43) Damager, I.; Numao, S.; Chen, H.; Brayer, G. D.; Withers, S. G. Synthesis and characterisation of novel chromogenic substrates for human pancreatic α-amylase. *Carbohydr. Res.* **2004**, *339* (10), 1727−1737.

https://doi.org/10.1021/acs.bioconjchem.5c00626
Bioconjugate Chem. XXXX, XXX, XXX−XXX